Breaking Orthogonality in Uplink with Heterogeneous Requirements and Randomly Deployed Sources

Apostolos A. Tegos*, Sotiris A. Tegos*†, Dimitrios Tyrovolas*,
Panagiotis D. Diamantoulakis*, Panagiotis Sarigiannidis†, George K. Karagiannidis*‡
*Department of Electrical and Computer Engineering, Aristotle University of Thessaloniki, 54124 Thessaloniki, Greece
e-mail: {apotegath, tegosoti, tyrovolas, padiaman, geokarag}@auth.gr
†Department of Informatics and Telecommunication Engineering, University of Western Macedonia, 50100 Kozani, Greece
e-mail: psarigiannidis@uowm.gr
‡Artificial Intelligence & Cyber Systems Research Center, Lebanese American University (LAU), Lebanon

2024 IEEE Wireless Communications and Networking Conference (WCNC) | 979-8-3503-0358-2/24/$31.00 ©2024 IEEE | DOI: 10.1109/WCNC57260.2024.10570690

***Abstract*—In sixth-generation (6G) wireless communication systems, the coexistence of enhanced mobile broadband (eMBB) and massive machine-type communications (mMTC) services requires the investigation of appropriate multiple access schemes. In this direction, this paper delves into the hybrid eMBB-mMTC policy, focusing on the implications of non-orthogonality in contention-based access schemes and combining the strengths of slotted ALOHA and successive interference cancellation to address the challenges of this hybrid policy. Closed-form expressions for the outage probability, which are crucial for deriving the throughput of the sources, are presented and integrated into a comprehensive analysis. Finally, simulation results are used to validate the provided theoretical expressions, highlighting the effects of random source deployment within the hybrid eMBB-mMTC framework and highlighting the potential and challenges of this policy in shaping the future of 6G wireless communication systems.**

***Index Terms*—random access, slotted ALOHA, NOMA, SIC, randomly distributed sources, outage probability, throughput, mMTC, eMBB**

I. Introduction

The evolution of sixth-generation (6G) wireless networks will build on the advances of 5G and delve deeper into areas such as enhanced mobile broadband (eMBB) and massive machine-type communications (mMTC) [1], [2]. As these networks evolve, the concept of network slicing emerges as a key strategy. This approach facilitates the dynamic allocation of resources, allowing them to be tailored to specific use cases and requirements. Such adaptability becomes critical when considering the diverse requirements of high-data-rate eMBB applications and the sporadic, massive connectivity of mMTC, especially in the context of the Internet of Things (IoT). The integration of these domains, as seen in hybrid policies, highlights the importance of developing advanced multiple access schemes to address the unique challenges they present.

In this context, the potential of power domain non-orthogonal multiple access (NOMA) over its orthogonal counterpart has been recognized [3]–[5]. This transition to NOMA highlights the importance of multi-user detection techniques. Successive interference cancellation (SIC), the foundation of NOMA, emerges as a key technique. It works by decoding the signal from a source, treating other signals as interference, and, upon successful decoding, subtracting the decoded signal from the superimposed received signal. This mechanism is particularly important in uplink NOMA, which offers an extended capacity region compared to orthogonal multiple access (OMA), potentially improving spectral efficiency [6], [7]. The integration of slotted ALOHA (SA) with SIC represents a promising solution to address network congestion and improve the efficiency of mMTC networks in hybrid scenarios [8]–[10]. However, the practical challenges, especially in the context of the hybrid eMBB-mMTC policy with its unique source deployment, require further investigation [11], [12]. To the best of the authors' knowledge, the intricacies of SA-SIC in such hybrid contexts remain underexplored.

Motivated by the challenges and potential of the hybrid eMBB-mMTC policy in the context of 6G networks, this work delves into the implications of non-orthogonality in a hybrid eMBB-mMTC scenario, especially when considering random source deployments. Specifically, the contributions of this work are as follows:

- In light of the complexities associated with breaking orthogonality in environments with random source deployment, a comprehensive policy for the hybrid eMBB-mMTC scenario has been formulated. For the evaluation of this policy's performance, we examine a scenario that employs the SA-SIC protocol, in which an eMBB device, located at a fixed location, shares its dedicated resource block with multiple mMTC devices that are randomly deployed within a ring.
- Closed-form expressions for the outage probability of the system, aligned with the aforementioned scenario, are presented. Using these expressions, the throughput of the sources for the hybrid eMBB-mMTC policy is derived.
- Finally, the provided theoretical expressions are validated through simulation results, emphasizing the effects of random source deployment within the hybrid eMBB-mMTC framework, from which valuable insights are derived for the design and optimization of such policies.

The remainder of this paper is organized as follows. The system model is described in Section II. The performance analysis of the considered network is presented in Section III and the numerical results are presented in Section IV. Finally, Section V concludes the paper.

II. System Model

We consider a network setup comprising a single-antenna base station (BS) with perfect channel state information (CSI) and N single-antenna sources. These sources transmit their signals within structured time intervals, as time is systematically segmented into frames. The received signal-to-noise ratio (SNR) for the i-th source can be represented as

$$\gamma_i = \frac{l_i |h_i|^2 p_i}{\sigma^2}, \tag{1}$$

where σ^2, h_i, and p_i represent the variance of the additive white Gaussian noise (AWGN), the small-scale fading coefficient between the i-th source and the base station (BS), and the transmitted power of the i-th source, respectively. Furthermore, the network's path loss factor is given by

$$l_i = c d_i^{-n}, \tag{2}$$

with c, d_i, and n being the path loss at reference distance d_0, the distance between the i-th source and the BS, and the path loss exponent, respectively. Under the assumption of Rayleigh fading, $|h_i|^2$ adheres to the exponential distribution with a rate parameter of 1, leading to γ_i following the exponential distribution with rate parameter $b_i = \frac{\sigma^2}{l_i p_i}$.

For a realistic representation of a network with randomly deployed sources, the sources are assumed to be uniformly distributed within a circular ring centered around the BS. The distance between the i-th source and the BS is modeled as a random variable with its cumulative distribution function (CDF) given as

$$F_{d_i}(x) = \frac{x^2 - r^2}{R^2 - r^2}, \ x \in [r, R], \tag{3}$$

and its probability density function (PDF) as

$$f_{d_i}(x) = \frac{2x}{R^2 - r^2}, \ x \in [r, R]. \tag{4}$$

By setting $r = 0$, the CDF and PDF for the scenario in which sources are uniformly distributed in a circular disk are derived, making the analysis general enough to encompass this case.

Within the hybrid eMBB-mMTC framework, the adoption of contention-based (CB) access schemes is driven by the need for flexible channel access. Specifically, CB schemes, characterized by their probabilistic approach, allow sources to access the channel, potentially leading to either single or multiple sources using the channel in any given time slot. Therefore, given the inherent unpredictability of CB access schemes, there is a pressing need for strategies that can effectively manage potential collisions and ensure uninterrupted communication. In this direction, the SA-SIC protocol, which combines the principles of SA and SIC, stands out as a promising solution, as it can address these challenges but also reduce collisions, and thus, enhance the network's reliability by managing interference from simultaneous transmissions. Specifically, this protocol can support up to two sources being active in the same time slot, while the simultaneous channel access by three or more sources leads to a collision. This is a notable upside of this protocol over conventional OMA protocols, such as SA, which can support only one source accessing the channel in each time slot.

Delving deeper into the SA-SIC protocol, at the start of each frame, the BS transmits a preamble packet. This packet aids in frame synchronization and informs sources about the available random access (RA) slots in that frame. To further clarify the RA mechanism, we consider the random variable $I_i \in \{0, 1\}$ defined as the outcome of a Bernoulli trial, where

$$I_i(t) = \begin{cases} 1, & \text{with probability } q_i \\ 0, & \text{with probability } 1 - q_i. \end{cases} \tag{5}$$

The access probability of I_i, represented as $\mathbb{E}[I_i] = q_i$, indicates a scenario where the i-th source transmits information in a specific time slot.

In the SA-SIC framework, the probability of K sources accessing the channel concurrently is determined by the cumulative outcome of N Bernoulli trials. This probability is given by the probability mass function of the Poisson binomial distribution

$$\Pr(K = k) = \sum_{A \in F_k} \prod_{i \in A} q_i \prod_{j \in A^c} (1 - q_i), \tag{6}$$

where F_k represents the set of all subsets of k integers chosen from $\{1, 2, ..., N\}$. In this setup, for scenarios where only the i-th source accesses the channel, the achievable rate is

$$R_i = B \log_2(1 + \gamma_i), \tag{7}$$

where B denotes the available bandwidth. However, given the competitive nature of channel access and the inherent characteristics of SA-SIC, the achievable rates for two simultaneous source transmissions are given as

$$R_{i,1} = B \log_2 \left(1 + \frac{\gamma_i}{\gamma_j + 1}\right). \tag{8}$$

If its message is decoded second, then the achievable rate is given by

$$R_{i,2} = B \log_2 \left(1 + \frac{\gamma_i}{\epsilon \gamma_j + 1}\right), \tag{9}$$

where $\epsilon \in \{0, 1\}$ represents the result of the first decoding. Specifically, $\epsilon = 1$, when the decoding of the j-th source is correct, while $\epsilon = 0$, if the first decoding fails.

III. Performance Analysis

In the hybrid eMBB-mMTC framework, it is essential to assess the network's reliability and performance, especially when considering the unique source deployment scenario and the SA-SIC protocol. Therefore, it is imperative to analyze the outage and throughput performance of the network in the presented context. In order to calculate the aforementioned metrics, it is necessary to define the threshold for the i-th source, which is expressed as

$$\beta_i = 2^{\frac{\hat{R}_i}{B}} - 1, \tag{10}$$

where $\hat{R}_i$ represents the target rate of the i-th source.

TABLE I: Cases for Φ_2.

Conditions		Term	Expressions
$\beta_i\beta_j \geq 1$	$d_j x > R$	Φ_2^{11}	$\frac{2}{R^2-r^2}\sum_{k=0}^{\infty}\binom{-1}{k}\left(\frac{p_i d_j^n}{p_j\beta_i}\right)^{-k}\frac{\gamma\left(\frac{nk+2}{n},\frac{\sigma^2\beta_i R^n}{cp_i}\right)-\gamma\left(\frac{nk+2}{n},\frac{\sigma^2\beta_i r^n}{cp_i}\right)}{n\left(\frac{\sigma^2\beta_i}{cp_i}\right)^{\frac{nk+2}{n}}}$
	$d_j x < r$	Φ_2^{21}	$\frac{2}{R^2-r^2}\sum_{k=0}^{\infty}\binom{-1}{k}\left(\frac{p_i d_j^n}{p_j\beta_i}\right)^{k+1}\frac{\gamma\left(\frac{2-nk-n}{n},\frac{\sigma^2\beta_i R^n}{cp_i}\right)-\gamma\left(\frac{2-nk-n}{n},\frac{\sigma^2\beta_i r^n}{cp_i}\right)}{n\left(\frac{\sigma^2\beta_i}{cp_i}\right)^{\frac{2-nk-n}{n}}}$
	$r < d_j x < R$	Φ_2^{31}	$\frac{2}{R^2-r^2}\sum_{k=0}^{\infty}\binom{-1}{k}\left(\frac{p_i d_j^n}{p_j\beta_i}\right)^{-k}\frac{\gamma\left(\frac{nk+2}{n},\frac{\sigma^2\beta_i (d_j x)^n}{cp_i}\right)-\gamma\left(\frac{nk+2}{n},\frac{\sigma^2\beta_i r^n}{cp_i}\right)}{n\left(\frac{\sigma^2\beta_i}{cp_i}\right)^{\frac{nk+2}{n}}}$ $+\frac{2}{R^2-r^2}\sum_{k=0}^{\infty}\binom{-1}{k}\left(\frac{p_i d_j^n}{p_j\beta_i}\right)^{k+1}\frac{\gamma\left(\frac{2-nk-n}{n},\frac{\sigma^2\beta_i R^n}{cp_i}\right)-\gamma\left(\frac{2-nk-n}{n},\frac{\sigma^2\beta_i (d_j x)^n}{cp_i}\right)}{n\left(\frac{\sigma^2\beta_i}{cp_i}\right)^{\frac{2-nk-n}{n}}}$
$\beta_i\beta_j < 1$	$d_j x > R$	Φ_2^{12}	$\Phi_2^{11}-\frac{2}{R^2-r^2}\sum_{k=0}^{\infty}\binom{-1}{k}\left(\frac{p_i d_j^n}{p_j\beta_i}\right)^{-k}e^{-\frac{\sigma^2\beta_j(\beta_i+1)d_j^n}{(1-\beta_i\beta_j)cp_j}}\frac{\gamma\left(\frac{nk+2}{n},\frac{\sigma^2\beta_i(\beta_j+1)R^n}{(1-\beta_i\beta_j)cp_i}\right)-\gamma\left(\frac{nk+2}{n},\frac{\sigma^2\beta_i(\beta_j+1)r^n}{(1-\beta_i\beta_j)cp_i}\right)}{n\left(\frac{\sigma^2\beta_i(\beta_j+1)}{(1-\beta_i\beta_j)cp_i}\right)^{\frac{nk+2}{n}}}$
	$d_j x < r$	Φ_2^{22}	$\Phi_2^{21}-\frac{2}{R^2-r^2}\sum_{k=0}^{\infty}\binom{-1}{k}\left(\frac{p_i d_j^n}{p_j\beta_i}\right)^{k+1}e^{-\frac{\sigma^2\beta_j(\beta_i+1)d_j^n}{(1-\beta_i\beta_j)cp_j}}\frac{\gamma\left(\frac{2-nk-n}{n},\frac{\sigma^2\beta_i(\beta_j+1)R^n}{(1-\beta_i\beta_j)cp_i}\right)-\gamma\left(\frac{2-nk-n}{n},\frac{\sigma^2\beta_i(\beta_j+1)r^n}{(1-\beta_i\beta_j)cp_i}\right)}{n\left(\frac{\sigma^2\beta_i(\beta_j+1)}{(1-\beta_i\beta_j)cp_i}\right)^{\frac{2-nk-n}{n}}}$
	$r < d_j x < R$	Φ_2^{32}	$\Phi_2^{31}-\frac{2}{R^2-r^2}\sum_{k=0}^{\infty}\binom{-1}{k}\left(\frac{p_i d_j^n}{p_j\beta_i}\right)^{-k}e^{-\frac{\sigma^2\beta_j(\beta_i+1)d_j^n}{(1-\beta_i\beta_j)cp_j}}\frac{\gamma\left(\frac{nk+2}{n},\frac{\sigma^2\beta_i(\beta_j+1)(d_j x)^n}{(1-\beta_i\beta_j)cp_i}\right)-\gamma\left(\frac{nk+2}{n},\frac{\sigma^2\beta_i(\beta_j+1)r^n}{(1-\beta_i\beta_j)cp_i}\right)}{n\left(\frac{\sigma^2\beta_i(\beta_j+1)}{(1-\beta_i\beta_j)cp_i}\right)^{\frac{nk+2}{n}}}$ $-\frac{2}{R^2-r^2}\sum_{k=0}^{\infty}\binom{-1}{k}\left(\frac{p_i d_j^n}{p_j\beta_i}\right)^{k+1}e^{-\frac{\sigma^2\beta_j(\beta_i+1)d_j^n}{(1-\beta_i\beta_j)cp_j}}\frac{\gamma\left(\frac{2-nk-n}{n},\frac{\sigma^2\beta_i(\beta_j+1)R^n}{(1-\beta_i\beta_j)cp_i}\right)-\gamma\left(\frac{2-nk-n}{n},\frac{\sigma^2\beta_i(\beta_j+1)(d_j x)^n}{(1-\beta_i\beta_j)cp_i}\right)}{n\left(\frac{\sigma^2\beta_i(\beta_j+1)}{(1-\beta_i\beta_j)cp_i}\right)^{\frac{2-nk-n}{n}}}$

A. Outage Probability

The following theorem provides the outage probability of the i-th source within the hybrid eMBB-mMTC scenario, considering the specific source deployment.

Theorem 1: The outage probability of the i-th source, when both i-th and j-th sources access the channel, is expressed as:

$$P_{ij} = \Phi_1 - \Phi_2 + \Phi_3 + \Phi_4, \tag{11}$$

where

$$\Phi_1 = 1 - e^{-\frac{\sigma^2\beta_j d_j^n}{cp_j}} \tag{12}$$

The expressions for Φ_2, Φ_3, and Φ_4 can be found in Tables I, II, and III, respectively. The variables x and y are defined as $x = \sqrt[n]{\frac{p_i}{\beta_i p_j}}$ and $y = \sqrt[n]{\frac{\beta_j p_i}{p_j}}$.

Proof: A detailed proof is available in Appendix A. ■

The primary condition in each table pertains to the product of the thresholds for each source, influencing the expression of (15), as detailed in Appendix A. The subsequent conditions in the tables, which the expressions rely upon, encompass all potential correlations between the distance d_j of the j-th source from the BS and the radii r and R of the ring where the i-th source is located.

B. Throughput Analysis

In the context of the hybrid eMBB-mMTC framework, it is essential to evaluate the throughput, especially considering the distinct source deployment and the SA-SIC access scheme. Specifically, in such scenarios where SA-SIC is employed, the throughput for the i-th source is expressed as

$$\begin{aligned}\tilde{R}_i &= \hat{R}_i q_i \prod_{k\neq i}(1-q_k)(1-P_i)\\ &\quad + \hat{R}_i q_i \sum_{j\neq i} q_j \prod_{k\neq i,j}(1-q_k)(1-P_{ij}),\end{aligned} \tag{13}$$

where P_i denotes the outage probability when only one source accesses the channel in a specific time slot. The outage probability when the i-th source is distributed in a circular ring and solely accesses the channel is given as

$$P_i = 1 - \frac{2}{R^2-r^2}\left(\frac{\gamma\left(\frac{2}{n},\frac{\sigma^2\beta_i R^n}{cp_i}\right)-\gamma\left(\frac{2}{n},\frac{\sigma^2\beta_i r^n}{cp_i}\right)}{n\left(\frac{\sigma^2\beta_i}{cp_i}\right)^{\frac{2}{n}}}\right). \tag{14}$$

IV. Numerical Results

In this section, we present the performance of the considered network and validate the derived expressions with simulations. We assume the path loss factor is given by (2), with $c = 10^{-3}$

TABLE II: Cases for Φ_3.

Conditions		Term	Expressions
$\beta_i\beta_j \geq 1$	$d_j y > R$	Φ_3^{11}	$\frac{2}{R^2-r^2}\sum_{k=0}^{\infty}\binom{-1}{k}\left(\frac{p_i\beta_j d_j^n}{p_j}\right)^{-k} e^{-\frac{\sigma^2\beta_j d_j^n}{cp_j}}\frac{R^{nk+2}-r^{nk+2}}{nk+2}$
	$d_j y < r$	Φ_3^{21}	$\frac{2}{R^2-r^2}\sum_{k=0}^{\infty}\binom{-1}{k}\left(\frac{p_i\beta_j d_j^n}{p_j}\right)^{k+1} e^{-\frac{\sigma^2\beta_j d_j^n}{cp_j}}\frac{R^{2-nk-n}-r^{2-nk-n}}{2-nk-n}$
	$r < d_j y < R$	Φ_3^{31}	$\frac{2}{R^2-r^2}\sum_{k=0}^{\infty}\binom{-1}{k}\left(\frac{p_i\beta_j d_j^n}{p_j}\right)^{-k} e^{-\frac{\sigma^2\beta_j d_j^n}{cp_j}}\frac{(d_j y)^{nk+2}-r^{nk+2}}{nk+2} + \frac{2}{R^2-r^2}\sum_{k=0}^{\infty}\binom{-1}{k}\left(\frac{p_i\beta_j d_j^n}{p_j}\right)^{k+1} e^{-\frac{\sigma^2\beta_j d_j^n}{cp_j}}\frac{R^{2-nk-n}-(d_j y)^{2-nk-n}}{2-nk-n}$
$\beta_i\beta_j < 1$	$d_j y > R$	Φ_3^{12}	$\Phi_3^{11}-\frac{2}{R^2-r^2}\sum_{k=0}^{\infty}\binom{-1}{k}\left(\frac{p_i\beta_j d_j^n}{p_j}\right)^{-k} e^{-\frac{\sigma^2\beta_j(\beta_i+1)d_j^n}{(1-\beta_i\beta_j)cp_j}}\frac{\gamma\left(\frac{nk+2}{n},\frac{\sigma^2\beta_i(\beta_j+1)R^n}{(1-\beta_i\beta_j)cp_i}\right)-\gamma\left(\frac{nk+2}{n},\frac{\sigma^2\beta_i(\beta_j+1)r^n}{(1-\beta_i\beta_j)cp_i}\right)}{n\left(\frac{\sigma^2\beta_i(\beta_j+1)}{(1-\beta_i\beta_j)cp_i}\right)^{\frac{nk+2}{n}}}$
	$d_j y < r$	Φ_3^{22}	$\Phi_3^{21}-\frac{2}{R^2-r^2}\sum_{k=0}^{\infty}\binom{-1}{k}\left(\frac{p_i\beta_j d_j^n}{p_j}\right)^{k+1} e^{-\frac{\sigma^2\beta_j(\beta_i+1)d_j^n}{(1-\beta_i\beta_j)cp_j}} \times\frac{\gamma\left(\frac{2-nk-n}{n},\frac{\sigma^2\beta_i(\beta_j+1)R^n}{(1-\beta_i\beta_j)cp_i}\right)-\gamma\left(\frac{2-nk-n}{n},\frac{\sigma^2\beta_i(\beta_j+1)r^n}{(1-\beta_i\beta_j)cp_i}\right)}{n\left(\frac{\sigma^2\beta_i(\beta_j+1)}{(1-\beta_i\beta_j)cp_i}\right)^{\frac{2-nk-n}{n}}}$
	$r < d_j y < R$	Φ_3^{32}	$\Phi_3^{31}-\frac{2}{R^2-r^2}\sum_{k=0}^{\infty}\binom{-1}{k}\left(\frac{p_i\beta_j d_j^n}{p_j}\right)^{-k} e^{-\frac{\sigma^2\beta_j(\beta_i+1)d_j^n}{(1-\beta_i\beta_j)cp_j}}\frac{\gamma\left(\frac{nk+2}{n},\frac{\sigma^2\beta_i(\beta_j+1)(d_j y)^n}{(1-\beta_i\beta_j)cp_i}\right)-\gamma\left(\frac{nk+2}{n},\frac{\sigma^2\beta_i(\beta_j+1)r^n}{(1-\beta_i\beta_j)cp_i}\right)}{n\left(\frac{\sigma^2\beta_i(\beta_j+1)}{(1-\beta_i\beta_j)cp_i}\right)^{\frac{nk+2}{n}}} -\frac{2}{R^2-r^2}\sum_{k=0}^{\infty}\binom{-1}{k}\left(\frac{p_i\beta_j d_j^n}{p_j}\right)^{k+1} e^{-\frac{\sigma^2\beta_j(\beta_i+1)d_j^n}{(1-\beta_i\beta_j)cp_j}}\frac{\gamma\left(\frac{2-nk-n}{n},\frac{\sigma^2\beta_i(\beta_j+1)R^n}{(1-\beta_i\beta_j)cp_i}\right)-\gamma\left(\frac{2-nk-n}{n},\frac{\sigma^2\beta_i(\beta_j+1)(d_j y)^n}{(1-\beta_i\beta_j)cp_i}\right)}{n\left(\frac{\sigma^2\beta_i(\beta_j+1)}{(1-\beta_i\beta_j)cp_i}\right)^{\frac{2-nk-n}{n}}}$

TABLE III: Cases for Φ_4.

Condition	Expressions
$d_j y > R$	$\frac{2}{R^2-r^2}\sum_{k=0}^{\infty}\binom{-1}{k}\left(\frac{p_i\beta_j d_j^n}{p_j}\right)^{-1-k} e^{-\frac{\sigma^2\beta_j d_j^n}{cp_j}}\frac{R^{nk+n+2}-r^{nk+n+2}}{nk+n+2} - \frac{2}{R^2-r^2}\sum_{k=0}^{\infty}\binom{-1}{k}\left(\frac{p_i\beta_j d_j^n}{p_j}\right)^{-1-k} e^{-\frac{\sigma^2\beta_j(\beta_i+1)d_j^n}{cp_j}}\frac{\gamma\left(\frac{nk+n+2}{n},\frac{\sigma^2\beta_i R^n}{cp_i}\right)-\gamma\left(\frac{nk+n+2}{n},\frac{\sigma^2\beta_i r^n}{cp_i}\right)}{n\left(\frac{\sigma^2\beta_i}{cp_i}\right)^{\frac{nk+n+2}{n}}}$
$d_j y < r$	$\frac{2}{R^2-r^2}\sum_{k=0}^{\infty}\binom{-1}{k}\left(\frac{p_i\beta_j d_j^n}{p_j}\right)^{k} e^{-\frac{\sigma^2\beta_j d_j^n}{cp_j}}\frac{R^{-nk+2}-r^{-nk+2}}{-nk+2} - \frac{2}{R^2-r^2}\sum_{k=0}^{\infty}\binom{-1}{k}\left(\frac{p_i\beta_j d_j^n}{p_j}\right)^{k} e^{-\frac{\sigma^2\beta_j(\beta_i+1)d_j^n}{cp_j}}\frac{\gamma\left(\frac{-nk+2}{n},\frac{\sigma^2\beta_i R^n}{cp_i}\right)-\gamma\left(\frac{-nk+2}{n},\frac{\sigma^2\beta_i r^n}{cp_i}\right)}{n\left(\frac{\sigma^2\beta_i}{cp_i}\right)^{\frac{-nk+2}{n}}}$
$r < d_j y < R$	$\frac{2}{R^2-r^2}\sum_{k=0}^{\infty}\binom{-1}{k}\left(\frac{p_i\beta_j d_j^n}{p_j}\right)^{-1-k} e^{\frac{\sigma^2\beta_j d_j^n}{cp_j}}\frac{(d_j y)^{nk+n+2}-r^{nk+n+2}}{nk+n+2} + \frac{2}{R^2-r^2}\sum_{k=0}^{\infty}\binom{-1}{k}\left(\frac{p_i\beta_j d_j^n}{p_j}\right)^{k} e^{\frac{\sigma^2\beta_j d_j^n}{cp_j}}\frac{R^{-nk+2}-(d_j y)^{-nk+2}}{-nk+2} - \frac{2}{R^2-r^2}\sum_{k=0}^{\infty}\binom{-1}{k}\left(\frac{p_i\beta_j d_j^n}{p_j}\right)^{-1-k} e^{-\frac{\sigma^2\beta_j(\beta_i+1)d_j^n}{cp_j}}\frac{\gamma\left(\frac{nk+n+2}{n},\frac{\sigma^2\beta_i (d_j y)^n}{cp_i}\right)-\gamma\left(\frac{nk+n+2}{n},\frac{\sigma^2\beta_i r^n}{cp_i}\right)}{n\left(\frac{\sigma^2\beta_i}{cp_i}\right)^{\frac{nk+n+2}{n}}} - \frac{2}{R^2-r^2}\sum_{k=0}^{\infty}\binom{-1}{k}\left(\frac{p_i\beta_j d_j^n}{p_j}\right)^{k} e^{-\frac{\sigma^2\beta_j(\beta_i+1)d_j^n}{cp_j}}\frac{\gamma\left(\frac{-nk+2}{n},\frac{\sigma^2\beta_i R^n}{cp_i}\right)-\gamma\left(\frac{-nk+2}{n},\frac{\sigma^2\beta_i (d_j y)^n}{cp_i}\right)}{n\left(\frac{\sigma^2\beta_i}{cp_i}\right)^{\frac{-nk+2}{n}}}$

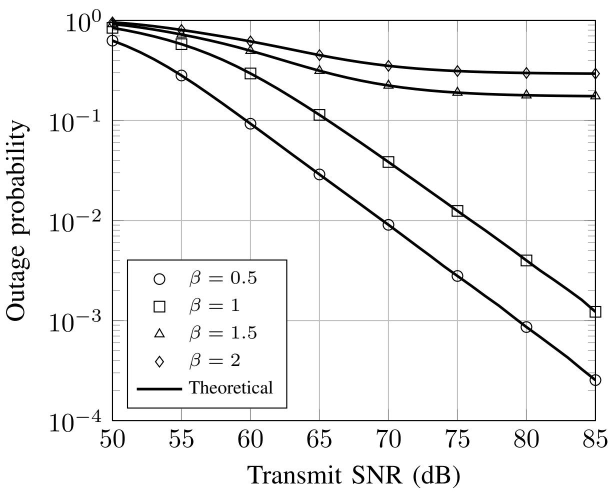

Fig. 1: Outage probability versus SNR.

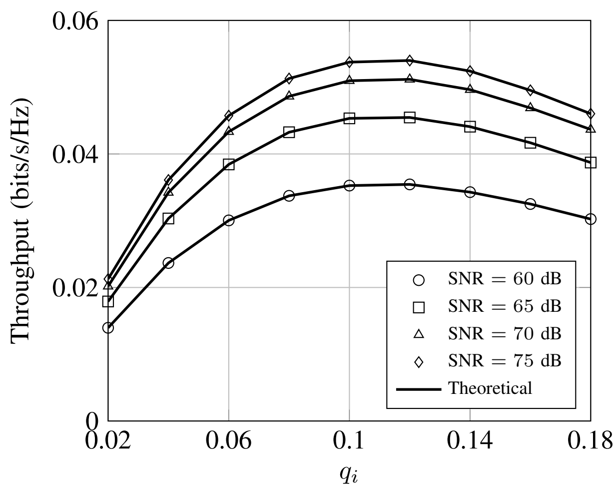

Fig. 2: System throughput versus q_i.

and $n = 2.5$. Furthermore, without loss of generality, it is assumed that the number of sources is $N = 10$, $N - 1$ are randomly deployed and 1 is located in a constant distance from the BS. The fixed user is always active, while the rest access the channel with a probability of $q_i = q_j = q_k = 1/N$, and $\beta_i = \beta_j = \beta = 2$ unless stated otherwise. It is assumed that $r_i = 5$ m, $R_i = 10$ m, and $d_j = 15$ m, where r_i and R_i denote the inner and outer radii of the ring in which the i-th source is uniformly distributed. Regarding the values of the SNR used in the simulations are concerned, the fact that transmit SNR is used justifies the values in the x-axes.

In Fig. 1, the outage probability of the i-th source versus the transmit SNR of the system is illustrated for various values of β, when two sources transmit simultaneously. As expected, lower threshold values correspond to lower outage probabilities, as does increasing the SNR. It should be highlighted that, for $\beta_i\beta_j > 1$, the outage probability is bounded by a minimum value, which is not the case for $\beta_i\beta_j \leq 1$.

In Fig. 2, the throughput versus q_i for the CB system is

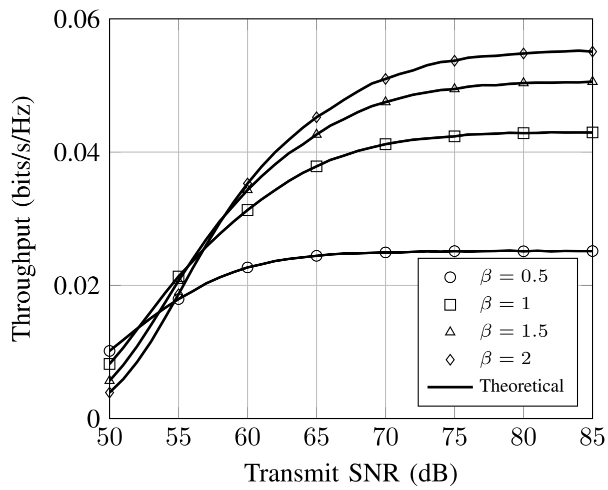

Fig. 3: Throughput versus SNR.

presented in the context of the hybrid eMBB-mMTC policy, offering insights across varying SNR values. This depiction is based on a scenario where $N - 1$ randomly distributed sources access the channel with a probability of q_i, complemented by a single, constantly active source at a fixed position. The system throughput, which primarily mirrors the performance of the randomly distributed sources, confirms the practical implications of the policy. As the transmit SNR increases, a notable increase in throughput is observed for consistent q_i values. Specifically, the system reaches its peak throughput at $q_i = 0.12$, but any increase beyond this point leads to a decline in throughput, which is attributed to the increased collision rate as the sources try to access the channel more frequently. A key takeaway from this figure is the observed stabilization of the maximum throughput as SNR values rise, indicating that a mere amplification of SNR might not always enhance throughput, particularly when considering the dynamics of the hybrid eMBB-mMTC policy.

Finally, in Fig. 3 the throughput of the network versus the transmit SNR is depicted, offering insights into the hybrid eMBB-mMTC policy's performance. As expected, the throughput increases for greater values of SNR, aligning with the simulation results for the outage probability. However, the influence of β on throughput presents an interesting contrast to its effect on the outage probability. Specifically, for small values of β, even though the outage probability decreases, the throughput does not display the anticipated increase. This observation can be explained by considering that higher SNR means greater power allocated to the correct message transmission, allowing the system to support higher transmission rates according to (10).

V. Conclusions

In this work, we investigated a hybrid eMBB/mMTC policy in 6G uplink wireless systems, highlighting the implications of non-orthogonality in CB access schemes. Our focus was on an RA protocol based on SA and SIC, termed SA-SIC, which is specifically designed for this hybrid policy. By deriving the outage probability and subsequently calculating the throughput for the system, we captured the dynamics of the hybrid eMBB/mMTC setting. Simulations were performed to validate our theoretical results while demonstrating the implications and challenges of the hybrid eMBB/mMTC policy. To this end, our work provides valuable design insights and underscores the importance of the hybrid eMBB/mMTC policy in shaping the future of 6G wireless systems.

Acknowledgment

This research has received funding from the European Union's Horizon Europe Framework Programme under grant agreement No 101096456.

Appendix A
Proof of Theorem 1

The outage probability of the i-th source, when two sources access the channel simultaneously and SIC is utilized as the detection technique for constant distances between the sources and the BS, is given by [8]

$$\begin{aligned} P_{ij} = \underbrace{1 - e^{-b_j \beta_j}}_{\phi_1} - \underbrace{\frac{b_j e^{-b_i \beta_i}}{b_i \beta_i + b_j} c_4}_{\phi_2} + \underbrace{\frac{b_j e^{b_i}}{\frac{b_i}{\beta_j} + b_j} c_5}_{\phi_3} \\ + \underbrace{\frac{b_i e^{-b_j \beta_j}}{b_j \beta_j + b_i} \left(1 - e^{-\beta_i (b_j \beta_j + b_i)}\right)}_{\phi_4}, \end{aligned} \tag{15}$$

where

$$c_4 = \begin{cases} 1 - e^{-(b_i \beta_i + b_j) \frac{(\beta_i + 1)\beta_j}{1 - \beta_i \beta_j}}, & \beta_i \beta_j < 1 \\ 1, & \beta_i \beta_j \geq 1 \end{cases} \tag{16}$$

and

$$c_5 = \begin{cases} e^{-\beta_j \left(\frac{b_i}{\beta_j} + b_j\right)} - e^{-\left(\frac{b_i}{\beta_j} + b_j\right) \frac{(\beta_i + 1)\beta_j}{1 - \beta_i \beta_j}}, & \beta_i \beta_j < 1 \\ e^{-\beta_j \left(\frac{b_i}{\beta_j} + b_j\right)}, & \beta_i \beta_j \geq 1. \end{cases} \tag{17}$$

To derive the outage probability, (15) should be integrated with respect to $d_i \in [r, R]$. Similar procedure is followed for all terms of (15), thus it is presented indicatively for the second term of (15), for which it stands that

$$\phi_2 = \begin{cases} \frac{\sigma^2 d_j^n}{c p_j} e^{-\frac{\sigma^2 \beta_i d_i^n}{c p_i}} \left(\frac{\sigma^2 \beta_i d_i^n}{c p_i} + \frac{\sigma^2 d_j^n}{c p_j} \right)^{-1}, & \beta_i \beta_j \geq 1 \\ \frac{\sigma^2 d_j^n}{c p_j} e^{-\frac{\sigma^2 \beta_i d_i^n}{c p_i}} \left(\frac{\sigma^2 \beta_i d_i^n}{c p_i} + \frac{\sigma^2 d_j^n}{c p_j} \right)^{-1} & \\ \times \left(1 - e^{-\frac{\beta_j (\beta_i + 1) \sigma^2 d_j^n}{(1 - \beta_i \beta_j) c p_j} - \frac{\beta_i \beta_j (\beta_i + 1) \sigma^2 d_i^n}{(1 - \beta_i \beta_j) c p_i}} \right), & \beta_i \beta_j < 1. \end{cases} \tag{18}$$

To integrate this expression, the negative binomial series is required, which arises in the binomial theorem for negative integer exponent and is given by

$$(x + a)^{-n} = \sum_{k=0}^{\infty} \binom{-n}{k} x^k a^{-n-k}, \tag{19}$$

TABLE IV: Negative binomial series.

Condition	Integral	Expression
$d_j x > R$	$\int_r^R \left(\frac{\sigma^2 d_j^n}{c p_j} + \frac{\sigma^2 \beta_i d_i^n}{c p_i} \right)^{-1} \mathrm{d}d_i$	$\sum_{k=0}^{\infty} \binom{-1}{k} \left(\frac{\sigma^2 d_j^n}{c p_j} \right)^{-k-1} \left(\frac{\sigma^2 \beta_i d_i^n}{c p_i} \right)^{k}$
$d_j x < r$	$\int_r^R \left(\frac{\sigma^2 d_j^n}{c p_j} + \frac{\sigma^2 \beta_i d_i^n}{c p_i} \right)^{-1} \mathrm{d}d_i$	$\sum_{k=0}^{\infty} \binom{-1}{k} \left(\frac{\sigma^2 d_j^n}{c p_j} \right)^{k} \left(\frac{\sigma^2 \beta_i d_i^n}{c p_i} \right)^{-k-1}$
$r < d_j x < R$	$\int_r^{d_j x} \left(\frac{\sigma^2 d_j^n}{c p_j} + \frac{\sigma^2 \beta_i d_i^n}{c p_i} \right)^{-1} \mathrm{d}d_i$	$\sum_{k=0}^{\infty} \binom{-1}{k} \left(\frac{\sigma^2 d_j^n}{c p_j} \right)^{-k-1} \left(\frac{\sigma^2 \beta_i d_i^n}{c p_i} \right)^{k}$
	$\int_{d_j x}^R \left(\frac{\sigma^2 d_j^n}{c p_j} + \frac{\sigma^2 \beta_i d_i^n}{c p_i} \right)^{-1} \mathrm{d}d_i$	$\sum_{k=0}^{\infty} \binom{-1}{k} \left(\frac{\sigma^2 d_j^n}{c p_j} \right)^{k} \left(\frac{\sigma^2 \beta_i d_i^n}{c p_i} \right)^{-k-1}$

for $|x| < a$. Considering the requirement for convergence during the integration, the cases presented in Table IV occur. Finally, utilizing [13, (3.381.8)], i.e.,

$$\int_0^u x^m e^{-\beta x^n} \mathrm{d}x = \frac{\gamma(\upsilon, \beta u^n)}{n \beta^{\upsilon}}, \tag{20}$$

where $\upsilon = \frac{m+1}{n}$, the final expressions are derived. Similarly, the rest of the terms are calculated, thus completing the proof.

References

[1] W. Saad, M. Bennis, and M. Chen, "A vision of 6G wireless systems: Applications, trends, technologies, and open research problems," *IEEE Netw.*, vol. 34, no. 3, pp. 134–142, May 2019.

[2] Z. Zhang, Y. Xiao, Z. Ma, M. Xiao, Z. Ding, X. Lei, G. K. Karagiannidis, and P. Fan, "6G wireless networks: Vision, requirements, architecture, and key technologies," *IEEE Veh. Technol. Mag.*, vol. 14, no. 3, pp. 28–41, Sep. 2019.

[3] Z. Ding, Z. Yang, P. Fan, and H. V. Poor, "On the performance of non-orthogonal multiple access in 5G systems with randomly deployed users," *IEEE Signal Process. Lett.*, vol. 21, no. 12, pp. 1501–1505, 2014.

[4] Z. Chen, Z. Ding, X. Dai, and G. K. Karagiannidis, "On the application of quasi-degradation to MISO-NOMA downlink," *IEEE Trans. Signal Process.*, vol. 64, no. 23, pp. 6174–6189, 2016.

[5] Z. Yang, Z. Ding, P. Fan, and G. K. Karagiannidis, "On the performance of non-orthogonal multiple access systems with partial channel information," *IEEE Trans. Commun.*, vol. 64, no. 2, pp. 654–667, 2016.

[6] Z. Wei, L. Yang, D. W. K. Ng, J. Yuan, and L. Hanzo, "On the performance gain of NOMA over OMA in uplink communication systems," *IEEE Trans. Commun.*, vol. 68, no. 1, pp. 536–568, 2020.

[7] P. D. Diamantoulakis, N. D. Chatzidiamantis, A. L. Moustakas, and G. K. Karagiannidis, "Next generation multiple access: Performance gains from uplink MIMO-NOMA," *IEEE Open J. Commun. Soc.*, vol. 3, pp. 2298–2313, 2022.

[8] S. A. Tegos, P. D. Diamantoulakis, A. S. Lioumpas, P. G. Sarigiannidis, and G. K. Karagiannidis, "Slotted ALOHA with NOMA for the next generation IoT," *IEEE Trans. Commun.*, vol. 68, no. 10, pp. 6289–6301, 2020.

[9] J. Choi, "NOMA-based Random Access with Multichannel Aloha," *IEEE J. Sel. Areas Commun.*, vol. 35, no. 12, pp. 2736–2743, 2017.

[10] ——, "Layered Non-Orthogonal Random Access With SIC and Transmit Diversity for Reliable Transmissions," *IEEE Trans. Commun.*, vol. 66, no. 3, pp. 1262–1272, 2018.

[11] N. Ehsan and R. L. Cruz, "On the optimal SINR in random access networks with spatial reuse," in *Proc. 40th Annual Conference on Information Sciences and Systems*, 2006, pp. 938–944.

[12] V. K. Papanikolaou, G. K. Karagiannidis, N. A. Mitsiou, and P. D. Diamantoulakis, "Closed-form analysis for NOMA with randomly deployed users in generalized fading," *IEEE Wireless Commun. Lett.*, vol. 9, no. 8, pp. 1253–1257, 2020.

[13] I. S. Gradshteyn and I. M. Ryzhik, *Table of integrals, series, and products*. Academic press, 2014.